Title: Seasonal gene-expression signatures of delayed fertilization in Fagaceae

Authors: Akiko Satake[1*], Kayoko Ohta[1], Noriko Takeda-Kamiya[2], Kiminori Toyooka[2], Junko Kusumi[3]

Affiliations:

[1] Department of Biology, Faculty of Science, Kyushu University, Fukuoka 819-0395, Japan.

[2] Technology Platform Division, Mass Spectrometry and Microscopy Unit, RIKEN Center for Sustainable Resource Science, Yokohama 230-0045, Japan

[3] Department of Environmental Changes, Faculty of Social and Cultural Studies, Kyushu University, Fukuoka 819-0395, Japan.

Abstract

In the family Fagaceae, fertilization is delayed by several weeks to one year after pollination, leading to one- or two-year fruiting species depending on whether fruiting occurs in the same or the next year after flowering. To investigate physiological responses underlying the regulation of delayed fertilization, we monitored seasonal changes in genome-wide gene expression in tissues including leaves and buds over two years under natural conditions in one- (*Quercus glauca*) and two-year fruiting species (*Lithocarpus edulis*). Genes associated with the responses to cold stress, photosynthesis, and cell proliferation, which are essential for survival and growth, showed highly conserved seasonal expression profiles regardless of species. However, seasonal expression profiles diverged between the one- and two-year fruiting species in genes associated with pollination, an important process contributing to the origin and maintenance of the reproductive barrier between plant species. By comparing seasonal progression of ovule development and gene expression in pistillate flowers, we revealed that ovules started developing after winter in the two-year fruiting species, which could be linked to the activation of genes involved in fertilization and female gametophyte development after winter. These findings suggest that the two-year fruiting species may have evolved a requirement of winter cold to prevent fertilization before winter and facilitate fertilization and embryo development in the following spring when temperature rises. This study offers new possibilities to explore the evolution of reproductive strategies in Fagaceae.

1 Introduction

Successful fertilization is the start of a new individual in sexual reproduction. In flowering plants, pollen grains (male gametophytes) arriving on the stigma germinate, and pollen tubes grow to fertilize the egg cell of the female gametophyte generally within 24 to 48 h or even less (Williams, 2008). However, a delay in fertilization more than 4 days was recorded over a century ago (Benson, 1894) and has since been reported in diverse taxa, including Fagales, Brassicales, Laurales and others (Sogo & Tobe, 2006). The family Fagaceae, the most diverse tree family in northern temperate regions, including oaks and beeches, contains an exceptional number of species with delayed fertilization (Satake & Kelly, 2021). A lapse in time between pollination and fertilization spans from several weeks to almost one year. Species in the genus *Fagus* fertilize their ovules five weeks after pollination (Sogo & Tobe, 2006), resulting in fruiting in the same year as flowering (one-year fruiting). In the genus *Lithocarpus*, 92% of 104 species ripen their fruits in the year after pollination (two-year fruiting; Satake & Kelly, 2021). The genus *Quercus* comprises a mixture of one- and two-year fruiting species (Satake & Kelly, 2021).

Satake & Kelly (2021) presented a hypothesis that explains the coevolution of flowering/fruiting phenology and delayed fertilization. They developed a mathematical model that takes into account the impact of winter seasons, which are unfavorable for reproduction, as well as competition for pollinators. By incorporating data on reproductive phenology, they were able to explore how these factors influence the evolution of fertilization timing. When flowering occurs late in the season, particularly during summer or fall, it can be challenging to achieve complete seed

maturation before the onset of the cold winter season for Fagaceae species that produce large acorns. The mathematical model has predicted that a strategy of delaying fertilization until after the winter season could evolve as a way to overcome this challenge (Satake and Kelly 2021). The theoretical prediction suggests that the appropriate response to seasonal environmental changes, particularly the response to cold winter, is important for adjusting the fertilization time and aligning it with other phenological traits such as flowering and fruiting time. However, little is known about what physiological responses underlie the regulation of fertilization timing and how they differ between one-year and two-year fruiting species.

The physiological responses to seasonal environmental changes can be studied at the molecular level using the molecular phenology approach (Kudoh, 2016), which monitors the seasonal dynamics of global gene expression profiles in leaves and buds under natural conditions. Recent technological advances in the field of genomics have made it possible to obtain time-course transcriptome data in natural settings in non-model organisms such as Fagaceae (Satake et al. 2022). Molecular phenology has been used to unravel gene expression patterns that govern plant phenology in a wide range of species, including herbs (Aikawa et al. 2010; Nagano et al., 2019, 2012; Richards et al., 2012; Satake et al., 2013), trees in temperate areas (Cronn et al., 2017; Jokipii-Lukkari et al., 2018; Lu, Gordon, Amarasinghe, & Strauss, 2020; Miyazaki et al., 2014; Satake, Kawatsu, Teshima, Kabeya, & Han, 2019), and trees in the tropics (Kobayashi et al., 2013; Yeoh et al., 2017).

To investigate gene-expression signature of delayed fertilization, here we present the comparative molecular phenology over two years in one- and two-year fruiting species of the

Fagaceae family. The one-year fruiting species is *Q. glauca* that starts blooming in April and fruits in the autumn in the same year as anthesis (Fig. 1a). The two-year fruiting species, *L. edulis,* begins flowering mainly in June with a minor flowering event in fall (Fig. S1) and fruits in the next year after flowering (Fig. 1b). Two genera, *Quercus* and *Lithocarpus*, diverged during the Paleocene (Manos & Stanford, 2001; Zhou et al., 2022) and diversified in North America and Asia, respectively. We show that performing comparative transcriptomics using these two genera in the same natural habitat is a powerful approach to identify evolutionary conservation and divergence of physiological responses to environmental changes.

2 Materials and Methods

2.1 Study site and sampling methods

The study site is in the biodiversity reserve of the Ito campus of Kyushu University (33°35′ 47.5″ N, 130°12′ 50.0″ E) situated in Fukuoka, southern Japan. The biodiversity reserve of the Ito campus occupies an area of approximately 37 ha at an elevation from 20 to 57 m a.s.l. The mean annual precipitation and temperature near the site are 1701.0 mm and 16.4 °C, respectively (Japan Meteorological Agency http://www.jma.go.jp/jma/indexe.html for 1991–2020). We studied two evergreen species, *Q. glauca* and *L. edulis*, which are endemic to Asia. The flowers are self-incompatible and wind-pollinated in *Q. glauca,* while they are animal pollinated in *L. edulis*.

We first characterized the seasonal dynamics of global transcriptomics every four weeks using a mixture of leaf and bud tissues over two years because molecular phenology data in floral tissues

are available for only several months in one-year fruiting species, which is too short to compare the seasonal progression of gene expression between species. To monitor the molecular phenology, we collected samples from three individuals each for *Q. glauca* (Q1, Q2, and Q3) and *L. edulis* (L1, L2, and L3; Fig. S2). The mean (± s.d.) diameter at breast height (DBH) of *Q. glauca* and *L. edulis* were 17.53 (±1.10) cm and 10.04 (±1.51) cm, respectively. We collected a pair of leaf and apical bud from three current-year shoots per individual every four weeks from May 2017 to February 2019 (sampling dates are provided in Table S1). The pistillate flowers were sampled from three branches per individual from June 2020 to June 2021 in *L. edulis* and from April 2021 to Jun 2021 in *Q. glauca* (Table S1). Samples were taken from the sun-exposed crown (approximately 4 m and 2 m from the ground for *Q. glauca* and *L. edulis*, respectively) using long pruning shears from 11:30 to 12:30 h. For each sample, 0.2–0.4 g of tissue was preserved in a 2 ml microtube containing 1.5 ml of RNA-stabilizing reagent (RNAlater; Ambion, Austin, TX, USA) immediately after harvesting. The samples were transferred to the laboratory within 3 hr after sampling, stored at 4 °C overnight and then stored at −80 °C until RNA extraction. During transport to the laboratory, the samples were kept in a cooler box with ice to maintain a low temperature.

2.2 RNA extraction

Total RNA was extracted in accordance with the method described in a previous study (Miyazaki et al., 2014). RNA was extracted independently from leaf and bud samples of each tree and pooled at each time point. Similarly, RNA was extracted independently from each pistillate flower sample.

RNA integrity was examined using the Agilent RNA 6000 Nano kit on a 2100 Bioanalyzer (Agilent Technologies), and the RNA yield was determined using a NanoDrop ND-2000 spectrophotometer (Thermo Fisher Scientific). The RNA integrity number (RIN) is listed in Table S2.

2.3 Generation of transcriptome next-generation sequencing (NGS) data

We obtained transcriptome data from our samples to design DNA microarray probes. We used eight samples collected monthly from one individual at the study site from May to December 2017 for *Q. glauca* and from June to December 2017 for *L. edulis* (Table S1). Five to six micrograms of total RNA (RNA mixed with equal amounts of RNA extracted from each of the leaves and buds of the same tree) was sent to Macrogen (South Korea), where a cDNA library was prepared with an Illumina TruSeq Sample Prep Kit, and paired-end transcriptome sequencing of each sample was conducted using an Illumina HiSeq2000 or NovaSeq6000 sequencer (Illumina, San Diego, CA, USA). A total of 299 and 313 million 100-bp paired-end reads were obtained for each species. De novo transcriptome assembly was conducted using Trinity version 2.0.6 (Grabherr et al., 2011). Read quality analysis was performed on the raw data using FastQC v0.11.7 (http://bioinformatics.babraham.ac.uk/projects/fastqc/). Quality trimming and adapter clipping were performed using Trimmomatic version 0.38 (Bolger, Lohse, & Usadel, 2014) to trim trailing bases below the average quality 15 and minimum length 36 and clip Illumina adapters. The resulting reads shorter than 50 bp were discarded. De novo transcriptome assembly was conducted using Trinity version 2.0.6 (Grabherr et al., 2011).

2.4 Probe design for the DNA microarray

For the custom microarray slides, we used the assembled sequences of the transcripts generated by the NGS described above. We selected the assembled sequences for array design based on two steps. We first extracted transcript sequences that showed high homology against *A. thaliana* (%Identity >= 40%, qcovhsp >= 40%) by BLASTX searches for each species. For each extracted transcript sequence, the top hit *A. thaliana* gene ID was selected. If multiple transcript sequences were annotated for the same *A. thaliana* gene ID, the longest transcript was selected. We obtained 19,290 and 19,426 transcript sequences for *Q. glauca* and *L. edulis*, respectively. In the second step, to select transcript sequences that are conserved across genera in the Fagaceae family, we extracted transcript sequences that were eliminated from the homology selection, but the sequence homology to *F. crenata* transcript sequences used for DNA microarray (Satake et al., 2019) was high (%Identity >= 60%, qcovhsp >= 60%, e-value cut-off: 10^{-5}) in BLASTX searches for each species. After the selection in step 2, we obtained additional 3,474 and 4,357 transcript sequences for *Q. glauca* and *L. edulis*, respectively. We pooled these transcript sequences for each species and designed the array using the e-array portal for array design hosted by Agilent (https://earray.chem.agilent.com/earray/) based on 22,764 and 23,783 transcript sequences for *Q. glauca* and *L. edulis*, respectively. Two probes were designed for each transcript sequence. After removing probes with redundant sequence, 42,121 and 42,436 probes were installed in the 8×60K array format.

2.5 Microarray analysis

One hundred nanograms of total RNA extracted from the leaves and buds of each sample was amplified, labelled, and hybridized to a 60K Agilent 60-mer oligomicroarray in accordance with the manufacturer's instructions for each sample for each time point based on the one-colour method. The hybridized microarray slides were scanned by an Agilent scanner. The relative hybridization intensities and background hybridization values were calculated using Agilent Feature Extraction Software (9.5.1.1). Among the two probes designed for each transcript sequence, we selected the probe with the largest median. Finally, we obtained time-series data of 15,451 and 15,182 independent probes for *Q. glauca* and *L. edulis*, respectively.

2.6 Prediction of orthologous genes

To identify orthologous genes across *Q. glauca* and *L. edulis*, we first used TransDecoder (http://transdecoder.sourceforge.net/) to detect coding regions from the RNA seq assembled contigs. To maximize the sensitivity to capture coding regions with functional significance, we scanned all coding regions detected by TransDecoder for the blastp or pfam searches. We used the protein sequence database of green plants (Viridiplantae) for homology searches with an e-value < 10^{-5}. Among the assembled contigs of *Q. glauca* and *L. edulis*, TransDecorder identified 101,371 and 86,128 contigs containing candidate coding regions with homology to known proteins. The longest predicted protein sequences of candidate coding regions were used for subsequent analysis. The construction of groups of orthologous genes (orthogroups, referred to here as gene families including

orthologue pairs) was performed for five plant species: *Q. glauca*, *L. edulis*, *Fagus crenata* (75,926 sequences reported in Satake et al. 2019) and *Q. robur* (25,808 sequences from OAK GENOME SEQUENCING http://www.oakgenome.fr), and *Arabidopsis thaliana* (48,359 sequences from TAIR https://www.arabidopsis.org).

The prediction of orthogroups was based on a blastp all-against-all comparison of the protein sequences (e-value < 10^{-5}) of these species, followed by clustering with OrthoFinder (Emms & Kelly, 2015, 2019). We obtained 32,149 orthogroups in total and then considered a pair of probes of the two species (*Q. glauca* and *L. edulis*) for which sequences belonged to an identical orthogroup to be orthologous genes. However, certain pairs of probes could not be assigned to be orthologous due to multiple partners within an orthogroup. Additionally, pairs of probes that belonged to an orthogroup lacking the sequence of *A. thaliana* were excluded due to the uncertainty of their function. Finally, we obtained 9,258 pairs of probes predicted to be orthologous genes (Table S3). The GO terms of predicted proteins (orthogroups) were retrieved from annotation data of *A. thaliana*. We removed probes with low signal and weak correlation between individuals using the following three criteria: (1) no signal over all time points, (2) the mean signal value over all time points is lower than 0.05, and (3) the mean of correlation between each pair of individuals is smaller than 0.2. A total of 7,707 pairs among the 9,258 pairs satisfied the criteria. We used time series data of these 7,707 probes for further analyses after normalization to a mean of zero and a standard deviation of one for each species.

2.7 Hierarchical clustering

194 To assess the similarity of the genome-wide transcriptional profiles across orthologous genes, we
195 performed hierarchical clustering using the monthly time series data of 7,707 orthologous genes from
196 March 2017 to February 2019. For each orthologous gene, there were 24 time points, with three
197 individuals each, for *Q. glauca* and *L. edulis*. We calculated the mean expression levels of each
198 orthologous gene across three individuals in each species and subsequently normalized the values by
199 adjusting the mean to zero and the standard deviation to one. We performed hierarchical clustering
200 using the Ward method and the Euclidian distance using the hclust function in R (ver. 3.6.1).
201

202 **2.8 Principal component analysis (PCA)**

203 To assess the seasonal expression dynamics of 7,707 orthologous genes, we performed PCA of the
204 gene expression profiles from all samples using the function prcomp of the stats package in R (ver
205 3.6.1). To investigate the genes and functions that most contribute to each principal component, we
206 extracted the top 2.5% of genes from the largest positive (n = 176) and negative loading values (n =
207 176) for each axis. Then, to test the enrichment of GO terms in each principal component, we
208 performed Fisher's exact tests (two-sided) using the fisher.test function in R (ver 3.6.1). After the
209 Fisher's exact tests, we controlled for the false discovery rate using Storey's Q-value method (Storey,
210 2002) and estimated the Q-value of each test using the qvalue package in R (ver 3.6.1). To test the
211 significance of the PCA loadings, we used the bootstrapped eigenvector method (Jackson, 1995;
212 Peres-Neto et al., 2003). Using this method, we confirmed that all the top 2.5% of genes with positive
213 or negative loading values that characterize each axis are considered significant contributors.

2.9 Gene ontology (GO) enrichment analysis

To inspect functions of genes for each cluster or those in the top 2.5% of genes that contribute to each of the three principal components, GO enrichment analysis was performed. The 7,707 orthologous genes were selected as a customized reference for the analysis. The list of GO terms for describing the biological process were retrieved from the Database for Annotation, Visualization, and Integrated Discovery (DAVID) (Dennis et al., 2003). Statistical tests for enrichment were performed using Fisher's exact tests (fisher.test function) in R (ver 3.6.1). We controlled for the false discovery rate using Storey's *Q*-value method (Storey, 2002) and estimated the *Q*-value of each test using the qvalue package in R (ver 3.6.1). The GO terms ~~from~~ with the top-5 lowest *P* value were selected for representation (Supplementary Tables 4 and 5).

2.10 Phylogenetic analysis

Based on GO enrichment analyses, we identified three candidate genes, *Secretary* (*SEC*)*5A* (AT1G76850), *SEC15B* (AT4G02350) and *RNA-dependent RNA polymerase 6* (*RDR6*: AT3G49500), that may contribute to the regulation of delayed fertilization. The phylogenetic tree for each of three genes was reconstructed based on the protein sequences of *A. thaliana*, *Oryza sativa*, three *Quercus* species, *L. edulis* and *F. crenata* with *Physcomitrella patens* ~~was used~~ as an outgroup. Sequences of *SEC5A*, *SEC15B*, and *RDR6* genes for *O. sativa*, *Q. suber,* and *P. patens* were obtained from OrthoDB release 10 (https://www.orthodb.org/) (Kriventseva et al., 2019). Database searches were conducted

using annotation keywords or identifiers of the TAIR database. The ortholog sequences of each gene were aligned using muscle implemented in MEGA X (Kumar et al., 2016). Maximum likelihood (ML) trees were constructed with 1,000 replicates for bootstrapping using RAxML v8.2.11 (Stamatakis, 2014) via raxmlGUI 2.0.10 platform (Edler, Klein, Antonelli, & Silvestro, 2021). For each ML estimation, the best substitution model was used, as determined by model testing conducted with ModelTest-NG version 0.1.7 (Darriba et al., 2020) via the raxmlGUI 2.0.10 (Edler et al., 2021). The resulting ML trees were visualized using Figtree version 1.44 (http://tree.bio.ed.ac.uk/software/figtree/).

2.11 RT–qPCR

Pistillate flower samples collected from *L. edulis* from June 2020 to June 2021 were used for RT–qPCR analysis. Because pistillate flowers are fertilized in a relatively short period in *Q. glauca*, we used pistillate flower samples from April 2021 to June 2021 for RT–qPCR analysis in *Q. glauca*. We quantified the expression levels of *SEC5A*, *SEC15B*, and *RDR6* using the expression level of *UBQ10* as a reference and the Bio-Rad CFX connect real-time PCR detection system (CRX96 Touch). cDNA synthesis was carried out using PrimeScript™ RT regent kit with gDNA Eraser (Takara, Japan) from 250 ng total RNA. The first strand cDNAs were diluted to 10 times for subsequent use. Gene specific real-time PCR was performed using 5 ng of cDNA and SsoFast™ EvaGreen® Supermix kit (Bio-Rad, Hercules, CA, USA) according to the manufacturer's instructions. The PCR condition was as follows: 95 ℃ for 2 min, followed by 40 cycles of 95 ℃ for 1 s, 60 ℃ for 5 s, and the fluorescent

signal was measured at the extension step. Melt curve analyses was carried out to validate the specificity of the PCR amplicons. All test cDNAs were run in duplicates for each gene, and the average was used for analysis. The relative expression level of *UBQ10* was normalized to the standard sample by using the comparative threshold cycle ($\Delta\Delta C_t$) method (Pfaffl, 2001). Gene specific primers were designed using Primer3 software (http://primer3.wi.mit.edu/), and confirmed by the observation of a single amplification product of the expected size and sequences. The PCR amplification efficiencies ranged from 102% for to 112% with $R^2 > 0.98$. At each time point, there are three biological replicates and two technical replicates for each species. We used *UBQ10* as a housekeeping gene because previous studies showed that the expression of *UBQ10* is stable in *F. crenata* (Miyazaki et al., 2014; Miyazaki & Satake, 2017). The mean (± s.d.) Ct values of *QgUBQ10* and *LeUBQ10* in pistillate flowers were 22.0 (± 0.51) and 24.75 (± 0.77), respectively. The primers used for RT–qPCR are listed in Table S4.

2.12 Histological analysis of ovule development

Pistillate flowers in different stages of development were fixed with 4% (w/v) formaldehyde, 2% (v/v) glutaraldehyde, and 0.05 M cacodylate buffer, dehydrated in an ethanol dilution series, and embedded in LR-white resin (Electron Microscopy Science). Sections (1-µm thick) were prepared with an ultramicrotome (Leica Microsystems EM-UC7) using a diamond knife (DIATOME Histo). Each section was stained with 0.05% (w/v) toluidine blue and observed with an upright light microscope with 20x objective lens (Olympus BX53 M and DP26 digital camera).

274

275 # 3 Results

276 ## 3.1 Winter and summer transcriptional profiles are distinctly different, but spring and

277 ## fall are similar

278 Our global transcriptomic data show clear seasonal dynamics (Fig. 2a). Most orthologues show highly

279 correlated seasonal expression profiles between species (mean of Pearson correlation = 0.39)

280 compared with those calculated from a set of randomly paired genes (mean of Pearson correlation =

281 0.0096; $P < 10^{-16}$; Wilcoxon test; Fig. S3). Hierarchical clustering of the monthly expression profiles

282 revealed clustering of winter months (December, January, February, March) and other seasons

283 regardless of species (Fig. 2a). The transcriptional profiles other than winter were divided into

284 summer months (June, July, August, and September) and spring (April, May, June) or fall (October

285 and November) (Fig. 2a). The expression profiles were similar between spring and fall regardless of

286 the different pheno-phases (bud burst and flowering in spring and fruiting in fall).

287

288 ## 3.2 Genome-wide molecular phenology is associated with seasonal change in

289 ## temperature, not for photoperiod and rainfall

290 We found a clear relationship between the transcriptional profiles and seasonal temperature change.

291 A winter transcriptional profile was observed when the mean temperature over the 2 weeks prior to

292 the monitoring date was lower than 11.3 °C (Fig. 2b), and summer transcriptional profiles appeared

293 when the mean temperature exceeded 22.7 °C. Between these temperature thresholds, spring and fall

294 transcriptional profiles were observed (Fig. 2b). The photoperiod and precipitation were not well
295 associated with seasonal transcriptional profiles (Fig. 2c, d). The photoperiod cannot be used to
296 distinguish the differences in transcriptional profiles between spring and summer or those between
297 fall and winter (Fig. 2c). Precipitation fluctuates heavily across months and years, which is different
298 from the seasonal transcriptional profiles (Fig. 2d). These results suggest that temperature is a major
299 driver of seasonal transcriptional dynamics.

300 Hierarchical clustering of the seasonal expression of individual genes showed that 1,942
301 genes were highly expressed only in winter (called winter genes) in both *L. edulis* and *Q. glauca*
302 (Cluster 1 in Fig. 3). The biological function of winter genes was enriched by Gene Ontology (GO)
303 terms associated with metabolism (Table S5), implying metabolic changes in response to winter cold.
304 A total of 1,566 genes were highly or moderately expressed in spring and fall (called spring-fall
305 genes) in both species (Cluster 2 in Fig. 3), in which GO terms associated with the cell cycle and cell
306 division were enriched (Table S5), suggesting active cell proliferation in spring or fall seasons. The
307 majority of genes (2,117 genes) were highly expressed in summer (called summer genes) in both
308 species (Cluster 3 in Fig. 3). The top GO term was “Oxidation–Reduction Process”, suggesting the
309 response to oxidative stress caused by high light and drought in summer (Table S5). The remaining
310 genes, which accounted for 27% of all orthologous genes, showed differential expression between
311 species (Fig. 3). A total of 1,004 genes were expressed in winter in *Q. glauca* but expressed in spring
312 and summer in *L. edulis* (called type 1 differentially expressed genes (DEGs); Cluster 4 in Fig. 3),
313 while 1,078 genes were expressed in winter in *L. edulis* but expressed in spring and summer in *Q.*

314 *glauca* (called type 2 DEGs; Cluster 5 in Fig. 3). The top five GO terms for type 1 and 2 DEGs
315 included "Oxidation–Reduction Process" and "Pollination", respectively (Table S5).
316
317 **3.3 Seasonal gene expression profiles are conserved for the cold stress response,**
318 **energy acquisition and cell proliferation but diverge for pollination across the two**
319 **species**
320 To identify and quantify the major axes of the seasonal gene expression profiles, we performed PCA.
321 We found that the first three axes of variation (the principal components; PCs) explain 41.3% of the
322 multidimensional functional space variation (Fig. 4a, b; Fig. S4). The first axis (PC1) accounted for
323 24.32% of the variation and distinguished gene expression profiles between winter and other seasons
324 (Fig. 4a, c). The second axis (PC2) accounted for 10.58% of the variation and separated ~~distinguishes~~
325 gene expression profiles between spring/fall and summer (Fig. 4a, d). Together, the first and second
326 axes represent conserved gene expression dynamics across the two species. In contrast, the third axis
327 (PC3) accounted for 6.45% of the variation and captured the differential gene expression dynamics
328 across the two species (Fig. 4b, e).
329 To identify the key genes responsible for defining each of the three axes, we selected the top
330 2.5% of genes (n = 176 for each axis) with the largest positive and negative loading values. This
331 selection was based on a validation of the significance of each gene's contribution to each axis. The
332 biological functions of the top 2.5% of genes that characterized the first axis with positive loading
333 were enriched by the GO term "Macromolecule Metabolic Process" (Table S6), which is consistent

with the GO term identified in the winter cluster Table S5). Genes associated with cold adaptation (e.g., *Arabidopsis thaliana DEAD-box RNA helicase*: *AtRH7:* AT5G62190) (Huang et al., 2016; Liu et al., 2016), freezing tolerance (e.g., *STARCH EXCESS 1*: *SEX1*: AT1G10760) (Yano et al., 2005; Yu et al., 2001), and proteome and RNA homeostasis (e.g., *Clp protease ATP-binding subunit*: *CLPC1*: AT5G50920) (Nishimura & Van Wijk, 2015; Sjögren, MacDonald, Sutinen, & Clarke, 2004) are included in this GO term (Fig. 5; Table S7), which suggests that the first axis is functionally characterized by the stress response to winter cold. The biological functions of the top 2.5% of genes that characterized the second axis with positive or negative loading were enriched in several GO terms associated with photosynthesis and cell division (Tables S6, S7). The genes associated with photosynthesis were highly expressed in summer (e.g., *STN7*: AT1G68830) (Bellaflore et al., 2005), and those associated with cell division showed an expression peak in spring (e.g., *A. thaliana RADiation54*: *AtRAD54*: AT3G19210 and *METHYLTRANSFERASE1: MET1*: AT5G49160; Fig. 5) (Kankel et al., 2003; Osakabe et al., 2006). This result suggests that the second axis is characterized by energy acquisition and growth. Increased expression of DNA repair and methylation in spring can be the response to DNA replication stress during leaf flushing and growth (Fig. 1). The slight delay in the expression peaks of *MET1* and *AtRAD54* in *L. edulis* (Fig. 5) can be explained by the delayed timing of leaf flushing in *L. edulis*.

The enriched GO terms for the top 2.5% of genes for the third axis with negative loading include “Cell Communications” and “Pollination” (Table S6), consistent with the GO term identified as Type 2 DEGs (Table S5). Because genes included in the GO term “Pollination” could be associated

with delayed fertilization, we conducted further analyses on these genes. All eight genes included in the GO term "Pollination" were found to overlap with the genes identified as Type 2 DEGs (Tables S5, S7). Among the eight genes, four genes encode membrane associated proteins, Niemann-Pick type C protein (NPC1-2: AT4G38350), G-type lectin S-receptor-like protein kinase (AT2G19130), and receptor-like protein kinase2 (RPK2: AT3G02130), and signal peptide peptidase (SPP: AT2G03120), involved in sphingolipid trafficking (Feldman, Poirier, & Lange, 2015), anther development (Mizuno et al., 2007), protein secretion (Han, Green, & Schnell, 2009) (Table S7). Purple acid phosphatase 15 (PAP15: AT3G07130) that is an acidic phosphatase with phytase activity (Kuang, Chan, Yeung, & Lim, 2009) was also included. The other three genes that are known to be associated with regulating fertilization on the female side in *A. thaliana.* Among the three genes, two are associated with exocytosis (*SEC5A* and *SEC15B*: Fig. 5). These genes encode subunits of the exocyst, an evolutionarily conserved heterooligomeric protein complex (Heider & Munson, 2012). The exocyst complex tethers and docks vesicles to target membranes (Guo et al., 1999). In *A. thaliana*, through an RNAi approach, these subunits of the exocyst complex were shown to be required for conferring stigma receptivity, suggesting the role of exocytosis as a crucial process during pollen acceptance (Safavian et al., 2015). The last gene is *RDR6* (Fig. 5), which functions in the biogenesis of trans-acting small interfering RNAs (ta-siRNAs) (Peragine, Yoshikawa, Wu, Albrecht, & Poethig, 2004; Yoshikawa, Peragine, Mee, & Poethig, 2005). Loss-of-function mutations in these genes exhibit an increased frequency of abnormal gamete precursors that often give rise to development of more than one female gametophyte in the Arabidopsis ovule (Olmedo-Monfil et al., 2010). Because

374 the association with fertilization has been most thoroughly investigated only in these three genes, we
375 selected *SEC5A*, *SEC15B*, and *RDR6* for further analysis. Because differential seasonal expression
376 profiles of these genes could be associated with the difference in the period of delay from pollination
377 to fertilization, we observed the ovule development by confocal microscopy and compared the ovule
378 development with the expression of *SEC5A*, *SEC15B*, and *RDR6* in pistillate flowers. Before the
379 analysis using pistillate flowers, we confirmed that the three genes of *Q. glauca* and *L. edulis* are
380 found in the clade of corresponding genes of other species in the molecular phylogenetic trees (Figs.
381 S5–S7).
382
383 **3.4 Ovules start developing after winter in two-year fruiting species**
384 The comparative anatomical investigation revealed that *L. edulis* takes 11 months to develop ovules,
385 which is six times longer than *Q. glauca*. In the pistillate flowers of *Q. glauca*, the locules are already
386 visible in May, which is one month after flowering and pollination (Fig. 6a). Six ovule primordia
387 were present, and two dome-shaped ovule primordia arose in each locule (Fig. 6a). These ovule
388 primordia expanded to fill the locules, and one megaspore mother cell was visible in the transverse
389 section in June (Fig. 6a). Because embryo development was observed in July (Fig. S8), fertilization
390 occurred between June and July in *Q. glauca*. In contrast, the pistillate flowers of *L. edulis* were
391 relatively unchanged over eight months after pollination. The three locules were visible, but the ovule
392 primordia were not yet differentiated in the transverse section in November (Fig. 6b). After winter,
393 two dome-shaped ovule primordia arose in each of three locules in March (Fig. 6b). It took an

394 additional two months for the ovules to be well differentiated with megaspore mother cells (Fig. 6b;
395 Fig. S9). In June, one ovule was successfully fertilized, and the zygote enlarged (Fig. 6b). The rest of
396 the ovules showed signs of abortion, as inner integuments and internal structures coagulated to form
397 amorphous, dark-staining structures contained within outer integuments (Fig. 6b).
398
399 **3.5 Expression of *SEC5A*, *SEC15B*, and *RDR6* in pistillate flowers increases after**
400 **winter in two-year fruiting species**
401 We compared the seasonal progression of ovule development with the expression profiles of *SEC5A*,
402 *SEC15b*, and *RDR6* in pistillate flowers quantified by RT–qPCR. The expression of these genes in *L.*
403 *edulis* peaked from March to May after winter (Fig. 6c), which is several months later than the peak
404 of leaf and bud tissues (Fig. 5) and coincides with the onset of ovule primordia development (Fig.
405 6b). The expression of *SEC5A* and *SEC15B* in *L. edulis* showed two other minor peaks in July and
406 October (Fig. 6c), suggesting the intermittent activation of exocytosis. The expression of *SEC5A* and
407 *RDR6* in *Q. glauca* was already high immediately after flowering in April and rapidly decreased in
408 May and June (Fig. 6c). In contrast, the expression level of *SEC15b* was low throughout the census
409 period (Fig. 6c), suggesting that *SEC15b* may be less important for fertilization in *Q. glauca*. Overall,
410 the consistency of expression dynamics and the onset of ovule development suggest that *SEC5A* and
411 *RDR6* are candidates for delayed fertilization in *L. edulis*.
412
413 **4 Discussion**

Our results demonstrate that a seasonal gene-expression signature of delayed fertilization is the activation of genes involved in fertilization and ovule development in response to low temperatures. This finding suggests that the two-year fruiting species may have evolved a requirement of winter cold to prevent fertilization before winter and allow for fertilization and embryo development in the following spring when temperature rise.

Our study also revealed evolutionary conserved mechanisms that facilitate appropriate physiological responses to seasonal environmental changes. Specifically, genes associated with the responses to cold stress, photosynthesis, and cell proliferation, which are essential for survival and growth, show highly conserved seasonal expression profiles regardless of species. This indicates that comparative transcriptomics in natural settings is a powerful approach for identifying evolutionary conservation and divergence of physiological responses to environmental changes.

Genes that exhibit divergent expression profiles between one- and two-year fruiting species could potentially be the candidate genes for delayed fertilization. In this study, our focus was on two genes, *SEC5A*, which encodes a subunit of the exocyst complex, and *RDR6*, which is required for posttranscriptional silencing. To validate the requirement of winter cold as an adaptive strategy for adjusting fertilization time, it would be useful to conduct female flower specific transcriptomics to see if their seasonal gene expression profiles are conserved in the two-year fruiting species and identify additional candidate genes of delayed fertilization.

The exocyst complex plays a critical role during pollen–stigma interactions by mediating the delivery of Golgi-derived secretory vesicles through vesicular trafficking, tethering, and fusion with

the plasma membrane for secretion (Cvrčková et al., 2012; Heider & Munson, 2012). The cargo of these secretory vesicles is unknown, but candidate cargo could be plasma membrane aquaporins, which could facilitate water transfer (Safavian & Goring, 2013; Windari et al., 2021) from the stigmatic papilla to the pollen grain for hydration and cell-wall modifying enzymes for stigmatic papillar cell wall loosening and pollen tube penetration (Elleman & Dickinson, 1996; Samuel et al., 2009). In two-year fruiting *Quercus* (*Q. acutissima*, *Q. rubra*, *Q. suber L.*, *Q. velutina*) pollen germinates instantly after pollination to penetrate the stigmatic surface to the stylar transmitting tissue (Cecich, 1997; Deng et al., 2022). Then, the pollen tube is arrested and overwinters at the style-joining site until the formation of the rudimentary ovule and embryo sac maturation in the next spring (Cecich, 1997; Deng et al., 2022). Intermittent and delayed activation of *SEC5A* in the pistillate flowers of *L. edulis* with a sharp expression peak after winter (Fig. 6c) implies female-side regulation for the delivery of secretory vesicles to provide the resources, probably cell-wall modifying enzymes or signalling molecules, necessary for the resumption of pollen tube growth to fertilize the ovule after a prolonged postpollination period. It will be interesting future studies to investigate the pollen tube growth dynamics and exocyst gene expression within the pistil and ovule in various species to elucidate the role of the exocyst complex in male and female gametophyte communication during the long journey from the pollen tube.

Another candidate for delayed fertilization is *RDR6*, which generates ta-siRNAs that essentially silence TEs, which are selfish genetic elements that insert copies of themselves into the genome, during female gametophyte development in Arabidopsis (Olmedo-Monfil et al., 2010). In

454 the pistillate flower of *L. edulis*, *RDR6* was highly expressed after winter, which was synchronized
455 with the timing of female gamete formation and the expression peak of *SEC5A*. These results show
456 that female gamete formation and pollen–pistil interactions are coordinately regulated in response to
457 seasonal environmental conditions, particularly the winter cold. ta-siRNAs are mobile signal
458 molecules that move from somatic cells into adjacent germline cells (Long et al., 2021; Martínez et
459 al., & Slotkin, 2016; Wu & Zheng, 2019) and even from host plants to fungal pathogens to induce
460 cross-species RNA interference (Cai et al., 2019; Cai et al., 2018). Because exocysts may participate
461 in tethering these extracellular vesicles to the plasma membrane (Saeed et al., 2019), it is tempting to
462 speculate that ta-siRNAs are actively delivered to silence TEs during gametogenesis to protect the
463 genome of the female gamete or enhance male and female gametophyte communication, probably
464 for the selection of compatible pollen tubes in Fagaceae with a high degree of self-incompatibility.
465 To gain a better understanding of how mobile siRNAs function in ovules of Fagaceae and to further
466 illuminate the roles of siRNAs in delayed fertilization, functional analyses and in-situ hybridization
467 experiments would be valuable strategies.

468 The long delay in fertilization has long been a mystery in biology. This study offers new
469 possibilities to explore the evolution of this unique reproductive strategies.

470

471 **Acknowledgements**

472 The authors would like to thank Y. Sawasaki and M. Seki for their supports in sample collection, M.
473 Seki and E. Sasaki for their technical supports with the statistical analysis, and K. Miwa for her

valuable comments on our initial draft. We also thank three reviews for their valuable suggestions to improve our manuscript.

References

Aikawa, S., Kobayashi, M. J., Satake, A., Shimizu, K. K., & Kudoh, H. (2010). Robust control of the seasonal expression of the Arabidopsis *FLC* gene in a fluctuating environment. *Proceedings of the National Academy of Sciences*, *107*(25), 11632–11637. doi: 10.1073/pnas.0914293107

Bellaflore, S., Barneche, F., Peltler, G., & Rochalx, J. D. (2005). State transitions and light adaptation require chloroplast thylakoid protein kinase STN7. *Nature*, *433*(7028), 892–895. doi: 10.1038/nature03286

Benson, M. (1894). Contribution to the embryology of the Amentiferae. Part I. *Transactions of the Linnean Society of London, 2nd Series, Botany*, *3*(R60), 409–424.

Boavida, L. C., Silva, J. P., & Feijó, J. A. (2011). Sexual reproduction in the cork oak (*Quercus suber L*). II. Crossing intra- and interspecific barriers. *Sexual Plant Reproduction*, *14*(3), 143–152. doi: 10.1007/s004970100100

Bolger, A. M., Lohse, M., & Usadel, B. (2014). Trimmomatic: A flexible trimmer for Illumina sequence data. *Bioinformatics*, *30*(15), 2114–2120. doi: 10.1093/bioinformatics/btu170

Borgardt, S. J., & Nixon, K. C. (2003). A comparative flower and fruit anatomical study of *Quercus acutissima*, a biennial-fruiting oak from the Cerris group (Fagaceae). *American Journal of Botany*, *90*(11), 1567–1584. doi: 10.3732/ajb.90.11.1567

Cai, Q., He, B., Weiberg, A., Buck, A. H., & Jin, H. (2019). Small RNAs and extracellular vesicles: New mechanisms of cross-species communication and innovative tools for disease control. *PLoS Pathogens*, *15*(12), 1–13. doi: 10.1371/journal.ppat.1008090

Cai, Q., Qiao, L., Wang, M., He, B., Lin, F., Palmquist, J., & Jin, H. (2018). Pathogen to silence virulence genes. *Science*, *360*(June), 1126–1129.

Cecich, R. A. (1997). Pollen tube growth in Quercus. *Forest Science*, *43*(1), 140–146.

Cronn, R., Dolan, P. C., Jogdeo, S., Wegrzyn, J. L., Neale, D. B., St. Clair, J. B., & Denver, D. R. (2017). Transcription through the eye of a needle: Daily and annual cyclic gene expression variation in Douglas-fir needles. *BMC Genomics*, *18*(1). doi: 10.1186/s12864-017-3916-y

Cvrčková, F., Grunt, M., Bezvoda, R., Hála, M., Kulich, I., Rawat, A., & Žárský, V. (2012). Evolution of the land plant exocyst complexes. *Frontiers in Plant Science*, *3*(JUL), 1–13. doi: 10.3389/fpls.2012.00159

Darriba, Di., Posada, D., Kozlov, A. M., Stamatakis, A., Morel, B., & Flouri, T. (2020). ModelTest-NG: A new and scalable tool for the selection of DNA and protein evolutionary models. *Molecular Biology and Evolution*, *37*(1), 291–294. doi: 10.1093/molbev/msz189

Deng, M., Yao, K., Shi, C., Shao, W., & Li, Q. (2022). Development of Quercus acutissima (Fagaceae) pollen tubes inside pistils during the sexual reproduction process. *Planta*, *256*(1), 1–15. doi: 10.1007/s00425-022-03937-9

Dennis, G., Sherman, B. T., Hosack, D. A., Yang, J., Gao, W., Lane, H. C., & Lempicki, R. A. (2003). DAVID: Database for annotation, visualization, and integrated discovery. *Genome Biology*, *4*(5). doi: 10.1186/gb-2003-4-9-r60

Edler, D., Klein, J., Antonelli, A., & Silvestro, D. (2021). raxmlGUI 2.0: A graphical interface and toolkit for phylogenetic analyses using RAxML. *Methods in Ecology and Evolution*, *12*(2), 373–377. doi: 10.1111/2041-210X.13512

Elleman, C. J., & Dickinson, H. G. (1996). Identification of pollen components regulating pollination-specific responses in the stigmatic papillae of *Brassica oleracea*. *New Phytologist*, *133*(2), 197–205. doi: 10.1111/j.1469-8137.1996.tb01886.x

Emms, D. M., & Kelly, S. (2015). OrthoFinder: solving fundamental biases in whole genome comparisons dramatically improves orthogroup inference accuracy. *Genome Biology*, *16*(1), 1–14. doi: 10.1186/s13059-015-0721-2

Emms, D. M., & Kelly, S. (2019). OrthoFinder: Phylogenetic orthology inference for comparative genomics. *Genome Biology*, *20*(1), 1–14. doi: 10.1186/s13059-019-1832-y

Feldman, M. J., Poirier, B. C., & Lange, B. M. (2015). Misexpression of the Niemann-Pick disease type C1 (NPC1)-like protein in Arabidopsis causes sphingolipid accumulation and reproductive defects. *Planta*, *242*(4), 921–933. doi: 10.1007/s00425-015-2322-4

Grabherr, M. G., Haas, B. J., Yassour, M., Levin, J. Z., Thompson, D. A., Amit, I., … Regev, A. (2011). Full-length transcriptome assembly from RNA-Seq data without a reference genome. *Nature Biotechnology*, *29*(7), 644–652. doi: 10.1038/nbt.1883

Guo, W., Roth, D., Walch-Solimena, C., & Novick, P. (1999). The exocyst is an effector for Sec4P, targeting secretory vesicles to sites of exocytosis. *EMBO Journal*, *18*(4), 1071–1080. doi: 10.1093/emboj/18.4.1071

Han, S., Green, L., & Schnell, D. J. (2009). The signal peptide peptidase is required for pollen function in arabidopsis. *Plant Physiology*, *149*(3), 1289–1301. doi: 10.1104/pp.108.130252

Heider, M. R., & Munson, M. (2012). Exorcising the Exocyst Complex. *Traffic*, *13*(7), 898–907. doi: 10.1111/j.1600-0854.2012.01353.x

Huang, C. K., Shen, Y. L., Huang, L. F., Wu, S. J., Yeh, C. H., & Lu, C. A. (2016). The DEAD-box RNA helicase AtRH7/PRH75 participates in pre-rRNA processing, plant development and cold tolerance in arabidopsis. *Plant and Cell Physiology*, *57*(1), 174–191. doi: 10.1093/pcp/pcv188

Jackson, D. A. (1995). Bootstrapped principal components analysis - Reply to Mehlman et al. *Ecology*, *76*(2), 644–645. doi: 10.2307/1941220

Jokipii-Lukkari, S., Delhomme, N., Schiffthaler, B., Mannapperuma, C., Prestele, J., Nilsson, O., … Tuominen, H. (2018). Transcriptional roadmap to seasonal variation in wood formation of Norway spruce. *Plant Physiology*, *176*(4), 2851–2870. doi: 10.1104/pp.17.01590

549 Kankel, M. W., Ramsey, D. E., Stokes, T. L., Flowers, S. K., Haag, J. R., Jeddeloh, J. A., …
550 Richards, E. J. (2003). Arabidopsis MET1 cytosine methyltransferase mutants. *Genetics*,
551 *163*(3), 1109–1122. doi: 10.1093/genetics/163.3.1109
552 Kobayashi, M. J., Takeuchi, Y., Kenta, T., Kume, T., Diway, B., & Shimizu, K. K. (2013). Mass
553 flowering of the tropical tree Shorea beccariana was preceded by expression changes in
554 flowering and drought-responsive genes. *Molecular Ecology*, *22*(18), 4767–4782. doi:
555 10.1111/mec.12344
556 Kriventseva, E. V., Kuznetsov, D., Tegenfeldt, F., Manni, M., Dias, R., Simão, F. A., & Zdobnov,
557 E. M. (2019). OrthoDB v10: Sampling the diversity of animal, plant, fungal, protist, bacterial
558 and viral genomes for evolutionary and functional annotations of orthologs. *Nucleic Acids*
559 *Research*, *47*(D1), D807–D811. doi: 10.1093/nar/gky1053
560 Kuang, R., Chan, K. H., Yeung, E., & Lim, B. L. (2009). Molecular and biochemical
561 characterization of AtPAP15, a purple acid phosphatase with phytase activity, in Arabidopsis.
562 *Plant Physiology*, *151*(1), 199–209. doi: 10.1104/pp.109.143180
563 Kudoh, H. (2016). Molecular phenology in plants: In natura systems biology for the comprehensive
564 understanding of seasonal responses under natural environments. *New Phytologist*, *210*(2),
565 399–412. doi: 10.1111/nph.13733
566 Kumar, S., Stecher, G., & Tamura, K. (2016). MEGA7: Molecular evolutionary genetics analysis
567 version 7.0 for bigger datasets. *Molecular Biology and Evolution*, *33*(7), 1870–1874. doi:
568 10.1093/molbev/msw054
569 Liu, Y., Tabata, D., & Imai, R. (2016). A cold-inducible DEAD-box RNA helicase from
570 *Arabidopsis thaliana* regulates plant growth and development under low temperature. *PLoS*
571 *ONE*, *11*(4), 1–21. doi: 10.1371/journal.pone.0154040
572 Long, J., Walker, J., She, W., Aldridge, B., Gao, H., Deans, S., … Feng, X. (2021). Nurse cell-
573 derived small RNAs define paternal epigenetic inheritance in Arabidopsis. *Science*, *373*(6550).
574 doi: 10.1126/science.abh0556
575 Lu, H., Gordon, M. I., Amarasinghe, V., & Strauss, S. H. (2020). Extensive transcriptome changes
576 during seasonal leaf senescence in field-grown black cottonwood (*Populus trichocarpa*
577 *Nisqually-1*). *Scientific Reports*, *10*(1), 1–14. doi: 10.1038/s41598-020-63372-2
578 Manos, P. S., & Stanford, A. M. (2001). The historical biogeography of Fagaceae: Tracking the
579 tertiary history of temperate and subtropical forests of the Northern Hemisphere. *International*
580 *Journal of Plant Sciences*, *162*(6 SUPPL.), S77–S93. doi: 10.1086/323280
581 Martínez, G., Panda, K., Köhler, C., & Slotkin, R. K. (2016). Silencing in sperm cells is directed by
582 RNA movement from the surrounding nurse cell. *Nature Plants*, *2*(4). doi:
583 10.1038/NPLANTS.2016.30
584 Miyazaki, Y., Maruyama, Y., Chiba, Y., Kobayashi, M. J., Joseph, B., Shimizu, K. K., … Satake,
585 A. (2014). Nitrogen as a key regulator of flowering in *Fagus crenata*: Understanding the
586 physiological mechanism of masting by gene expression analysis. *Ecology Letters*, *17*(10),
587 1299–1309. doi: 10.1111/ele.12338

588 Miyazaki, Y., & Satake, A. (2017). Relationship between seasonal progression of floral meristem
589 development and *FLOWERING LOCUS T* expression in the deciduous tree Fagus crenata.
590 *Ecological Research*, *32*(4), 627–631. doi: 10.1007/s11284-017-1462-3
591 Mizuno, S., Osakabe, Y., Maruyama, K., Ito, T., Osakabe, K., Sato, T., … Yamaguchi-Shinozaki,
592 K. (2007). Receptor-like protein kinase 2 (RPK 2) is a novel factor controlling anther
593 development in Arabidopsis thaliana. *Plant Journal*, *50*(5), 751–766. doi: 10.1111/j.1365-
594 313X.2007.03083.x
595 N Saitou, M. N. (1987). The neighbor-joining method: a new method for reconstructing
596 phylogenetic trees. *Molecular Biol Ogy and Evolution*, *4*(4), 406–425. doi: doi: 10.1093/
597 Nagano, A. J., Kawagoe, T., Sugisaka, J., Honjo, M. N., Iwayama, K., & Kudoh, H. (2019). Annual
598 transcriptome dynamics in natural environments reveals plant seasonal adaptation. *Nature*
599 *Plants*, *5*(1), 74–83. doi: 10.1038/s41477-018-0338-z
600 Nagano, A. J., Sato, Y., Mihara, M., Antonio, B. A., Motoyama, R., Itoh, H., … Izawa, T. (2012).
601 Deciphering and prediction of transcriptome dynamics under fluctuating field conditions. *Cell*,
602 *151*(6), 1358–1369. doi: 10.1016/j.cell.2012.10.048
603 Nishimura, K., & Van Wijk, K. J. (2015). Organization, function and substrates of the essential Clp
604 protease system in plastids. *Biochimica et Biophysica Acta - Bioenergetics*, *1847*(9), 915–930.
605 doi: 10.1016/j.bbabio.2014.11.012
606 Olmedo-Monfil, V., Durán-Figueroa, N., Arteaga-Vázquez, M., Demesa-Arévalo, E., Autran, D.,
607 Grimanelli, D., … Vielle-Calzada, J. P. (2010). Control of female gamete formation by a small
608 RNA pathway in Arabidopsis. *Nature*, *464*(7288), 628–632. doi: 10.1038/nature08828
609 Osakabe, K., Abe, K., Yoshioka, T., Osakabe, Y., Todoriki, S., Ichikawa, H., … Toki, S. (2006).
610 Isolation and characterization of the *RAD54* gene from *Arabidopsis thaliana*. *Plant Journal*,
611 *48*(6), 827–842. doi: 10.1111/j.1365-313X.2006.02927.x
612 Peragine, A., Yoshikawa, M., Wu, G., Albrecht, H. L., & Poethig, R. S. (2004). SGS3 and
613 SGS2/SDE1/RDR6 are required for juvenile development and the production of trans-acting
614 siRNAs in Arabidopsis. *Genes and Development*, *18*(19), 2368–2379. doi:
615 10.1101/gad.1231804
616 Peres-Neto, P. R., Jackson, D. A., & Somers, K. M. (2003). Giving meaningful interpretation to
617 ordination axes: Assessing loading significance in principal component analysis. *Ecology*,
618 *84*(9), 2347–2363. doi: 10.1890/00-0634
619 Pfaffl, M. W. (2001). A new mathematical model for relative quantification in real-time RT-PCR.
620 *Nucleic Acids Research*, *29*(9), E45. doi: 10.1093/NAR/29.9.E45
621 Richards, C. L., Rosas, U., Banta, J., Bhambhra, N., & Purugganan, M. D. (2012). Genome-wide
622 patterns of Arabidopsis gene expression in nature. *PLoS Genetics*, *8*(4). doi:
623 10.1371/journal.pgen.1002662
624 Saeed, B., Brillada, C., & Trujillo, M. (2019). Dissecting the plant exocyst. *Current Opinion in*
625 *Plant Biology*, *52*, 69–76. doi: 10.1016/j.pbi.2019.08.004

626 Safavian, D., & Goring, D. R. (2013). Secretory activity is rapidly induced in stigmatic papillae by
627 compatible pollen, but inhibited for self-incompatible pollen in the brassicaceae. *PLoS ONE*,
628 *8*(12). doi: 10.1371/journal.pone.0084286
629 Safavian, D., Zayed, Y., Indriolo, E., Chapman, L., Ahmed, A., & Goring, D. R. (2015). RNA
630 silencing of exocyst genes in the stigma impairs the acceptance of compatible pollen in
631 arabidopsis. *Plant Physiology*, *169*(4), 2526–2538. doi: 10.1104/pp.15.00635
632 Samuel, M. A., Chong, Y. T., Haasen, K. E., Aldea-Brydges, M. G., Stone, S. L., & Goring, D. R.
633 (2009). Cellular pathways regulating responses to compatible and self-incompatible pollen in
634 brassica and arabidopsis stigmas intersect at exo70a1, a putative component of the exocyst
635 complex. *Plant Cell*, *21*(9), 2655–2671. doi: 10.1105/tpc.109.069740
636 Satake, A., Kawagoe, T., Saburi, Y., Chiba, Y., Sakurai, G., & Kudoh, H. (2013). Forecasting
637 flowering phenology under climate warming by modelling the regulatory dynamics of
638 flowering-time genes. *Nature Communications*, *4*, 1–8. doi: 10.1038/ncomms3303
639 Satake, A., Kawatsu, K., Teshima, K., Kabeya, D., & Han, Q. (2019). Field transcriptome revealed
640 a novel relationship between nitrate transport and flowering in Japanese beech. *Scientific*
641 *Reports*, *9*(1), 1–12. doi: 10.1038/s41598-019-39608-1
642 Satake, A., & Kelly, D. (2021). Delayed fertilization facilitates flowering time diversity in
643 Fagaceae. *Philosophical Transactions of the Royal Society B: Biological Sciences*, *376*(1839),
644 20210115. doi: 10.1098/rstb.2021.0115
645 Satake, A., Nagahama, A., & Sasaki, E. (2022). A cross-scale approach to unravel the molecular
646 basis of plant phenology in temperate and tropical climates. *New Phytologist*, *233*(6), 2340–
647 2353. doi: 10.1111/nph.17897
648 Sjögren, L. L. E., MacDonald, T. M., Sutinen, S., & Clarke, A. K. (2004). Inactivation of the clpC1
649 gene encoding a chloroplast Hsp100 molecular chaperone causes growth retardation, leaf
650 chlorosis, lower photosynthetic activity, and a specific reduction in photosystem content. *Plant*
651 *Physiology*, *136*(4), 4114–4126. doi: 10.1104/pp.104.053835
652 Sogo, A., & Tobe, H. (2006). Delayed fertilization and pollen-tube growth in pistils of *Fagus*
653 *japonica* (Fagaceae). *American Journal of Botany*, *93*(12), 1748–1756. doi:
654 10.3732/ajb.93.12.1748
655 Stamatakis, A. (2014). RAxML version 8: A tool for phylogenetic analysis and post-analysis of
656 large phylogenies. *Bioinformatics*, *30*(9), 1312–1313. doi: 10.1093/bioinformatics/btu033
657 Storey, J. D. (2002). A direct approach to false discovery rates. *Journal of the Royal Statistical*
658 *Society. Series B: Statistical Methodology*, *64*(3), 479–498. doi: 10.1111/1467-9868.00346
659 Williams, J. H. (2008). Novelties of the flowering plant pollen tube underlie diversification of a key
660 life history stage. *Proceedings of the National Academy of Sciences of the United States of*
661 *America*, *105*(32), 11259–11263. doi: 10.1073/pnas.0800036105
662 Windari, E. A., Ando, M., Mizoguchi, Y., Shimada, H., Ohira, K., Kagaya, Y., … Suwabe, K.
663 (2021). Two aquaporins, sip1;1 and pip1;2, mediate water transport for pollen hydration in the
664 arabidopsis pistil. *Plant Biotechnology*, *38*(1), 77–87. doi:
665 10.5511/plantbiotechnology.20.1207a

Wu, W., & Zheng, B. (2019). Intercellular delivery of small RNAs in plant gametes. *New Phytologist*, *224*(1), 86–90. doi: 10.1111/nph.15854

Yano, R., Nakamura, M., Yoneyama, T., & Nishida, I. (2005). Starch-related α-glucan/water dikinase is involved in the cold-induced development of freezing tolerance in Arabidopsis. *Plant Physiology*, *138*(2), 837–846. doi: 10.1104/pp.104.056374

Yeoh, S. H., Satake, A., Numata, S., Ichie, T., Lee, S. L., Basherudin, N., … Tani, N. (2017). Unravelling proximate cues of mass flowering in the tropical forests of South-East Asia from gene expression analyses. *Molecular Ecology*, *26*(19), 5074–5085. doi: 10.1111/mec.14257

Yoshikawa, M., Peragine, A., Mee, Y. P., & Poethig, R. S. (2005). A pathway for the biogenesis of trans-acting siRNAs in Arabidopsis. *Genes and Development*, *19*(18), 2164–2175. doi: 10.1101/gad.1352605

Yu, T. S., Kofler, H., Häusler, R. E., Hille, D., Flügge, U. I., Zeeman, S. C., … Weber, A. (2001). The Arabidopsis sex1 mutant is defective in the R1 protein, a general regulator of starch degradation in plants, and not in the chloroplast hexose transporter. *Plant Cell*, *13*(8), 1907–1918. doi: 10.1105/tpc.13.8.1907

Zhou, B. F., Yuan, S., Crowl, A. A., Liang, Y. Y., Shi, Y., Chen, X. Y., … Wang, B. (2022). Phylogenomic analyses highlight innovation and introgression in the continental radiations of Fagaceae across the Northern Hemisphere. *Nature Communications*, *13*(1), 1–14. doi: 10.1038/s41467-022-28917-1

Data Accessibility and Benefit-Sharing

The sequence data and DNA microarray data that support the findings of this study are available from the NCBI BioProject (accession PRJNA872835 for *Q. glauca* and PRJNA872836 for *L. edulis*), the NCBI Shotgun Assembly Sequence Database (TSA) (accession GKBD00000000 for *Q. glauca* and GKBC00000000 for *L. edulis*), and the NCBI GEO database (accession GSE211382, GSE211384, and GSE211385). Benefits from this research accrue from the sharing of our data and results on public databases as described above.

Author contributions

A.S. conceived of and designed the analysis; K.O. and A.S. collected samples; and K.O. performed the molecular experiments. K.J. and A.S. analysed the data; N.T. and K.T. performed anatomical observation of ovules. A.S. wrote the paper with input from all of the authors. This study was funded by JSPS KAKENHI (JP17H01449, JP21H04781) to A.S.

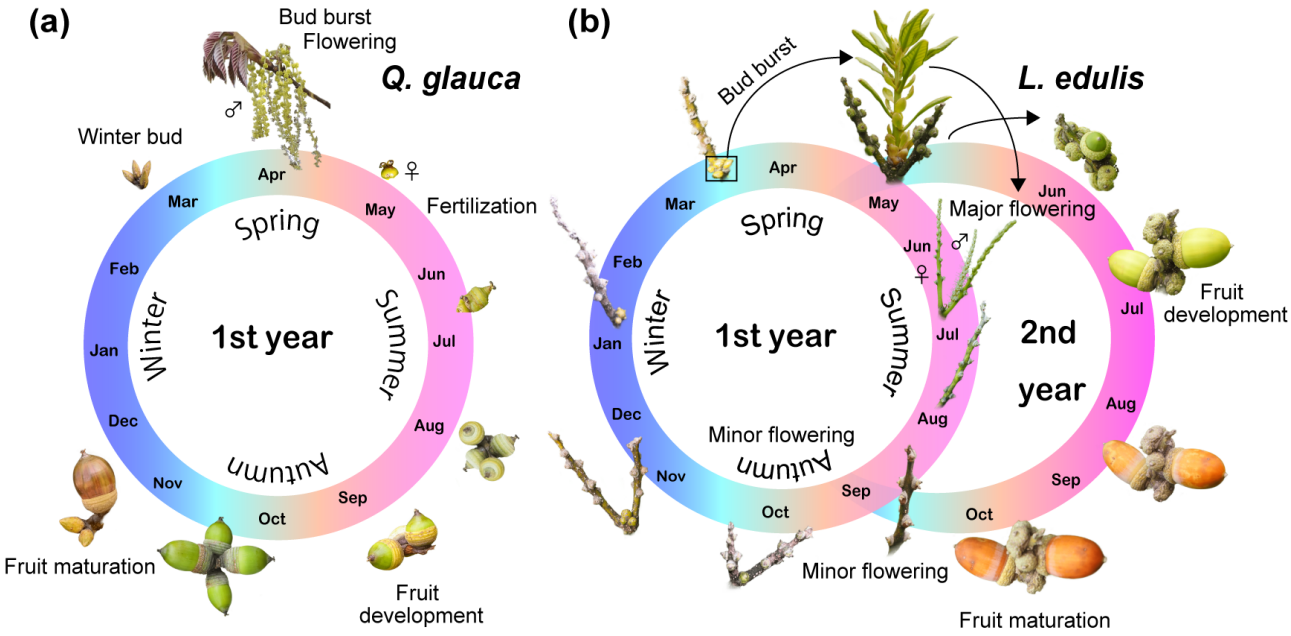

FIGURE 1 Comparison of flowering and fruiting phenology of *Q. glauca* and *L. edulis*. (a) A one-year fruiting species, *Q. glauca*, starts blooming in April and fruits in the autumn in the same year as anthesis. (b) A two-year fruiting species, *L. edulis*, begins flowering mainly in June with a minor flowering event in fall and fruits in the next year after flowering.

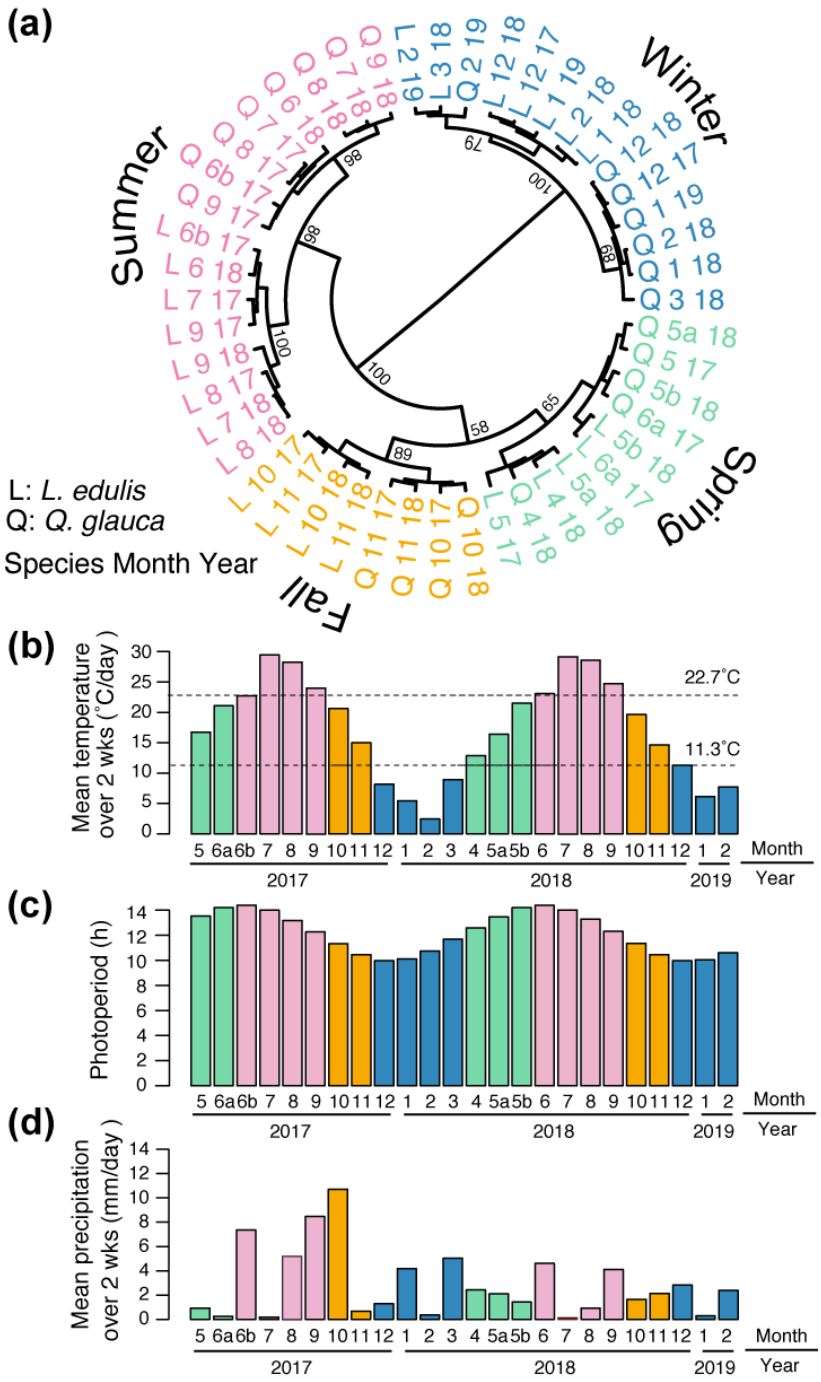

FIGURE 2 Molecular phenology and seasonal environmental changes. (a) Hierarchical clustering of monthly transcriptome profiles of tissues including leaves and buds in *Q. glauca* (Q) and *L. edulis* (L). The numbers indicate the month and year when each sample was collected. When sampling was performed twice a year, the month is distinguished by a or b (Table S1). The number given to each branch represents the bootstrap confidence level from 1,000 bootstrap samples. (b) The mean temperature over two weeks before the sampling dates. Dashed lines represent 22.7 °C, above which temperature the summer profiles in gene expression emerge, and 11.3 °C, below which temperature the winter profiles in gene expression emerge. (c) The photoperiod on sampling dates. (d) The mean precipitation over two weeks before the sampling dates. The colours in Panels (b), (c), and (d) indicate the gene expression profiles for winter (blue), spring (green), summer (pink), and fall (orange), which are consistent with those in Panel (a).

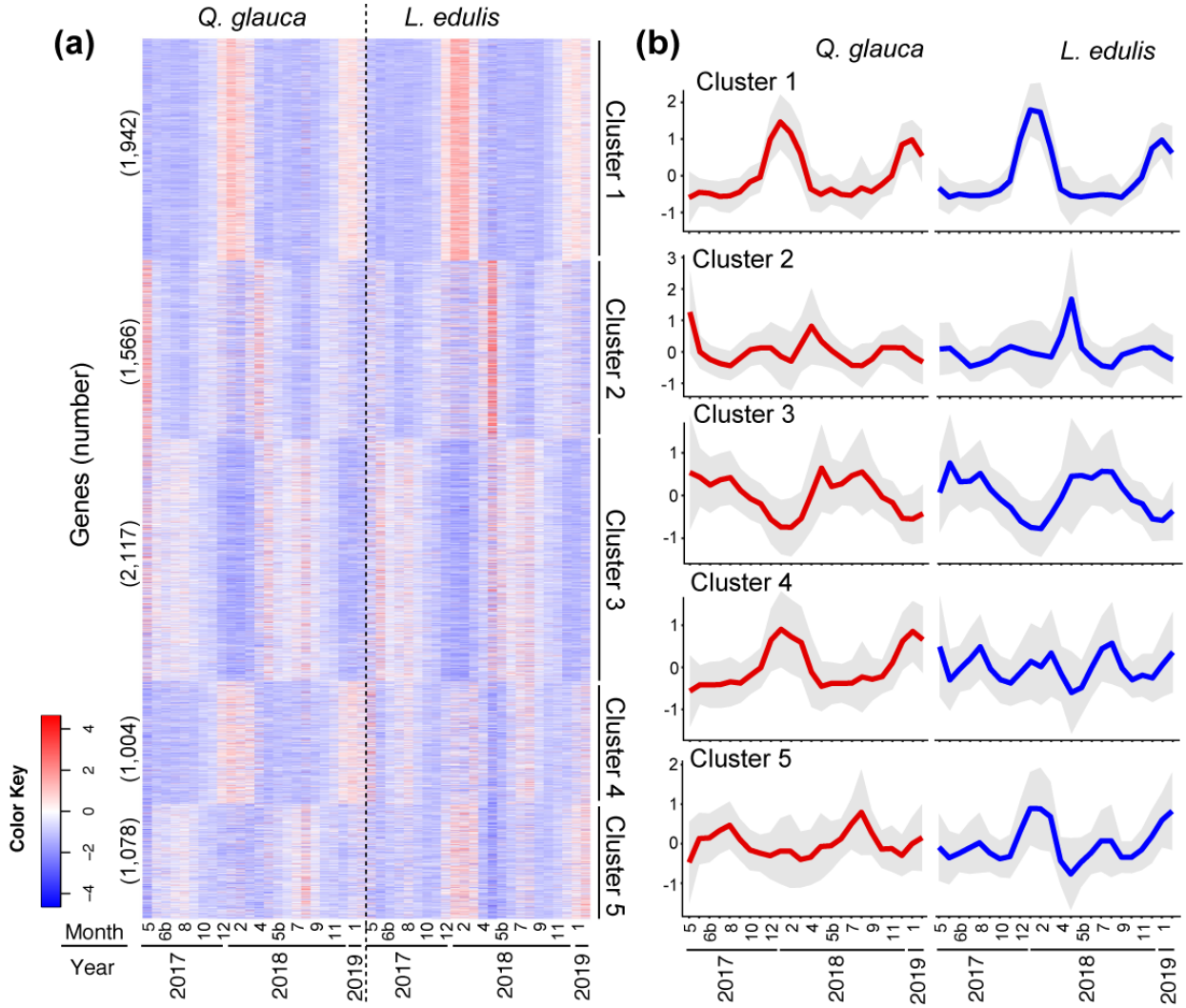

FIGURE 3 Five representative clusters for seasonal expression profiles of 7,707 orthologues. (a) A hierarchically clustered heatmap of seasonal expression profiles of 7,707 orthologues in tissues including leaves and buds. The numbers in brackets indicate the number of genes included in each cluster. (b) Seasonal expression profiles of genes in each of the five clusters. The average (line) ± s.d. (envelope) is shown (n = 1,942, 1,556, 2,117, 1,004, and 1,078 for Cluster 1–5, respectively).

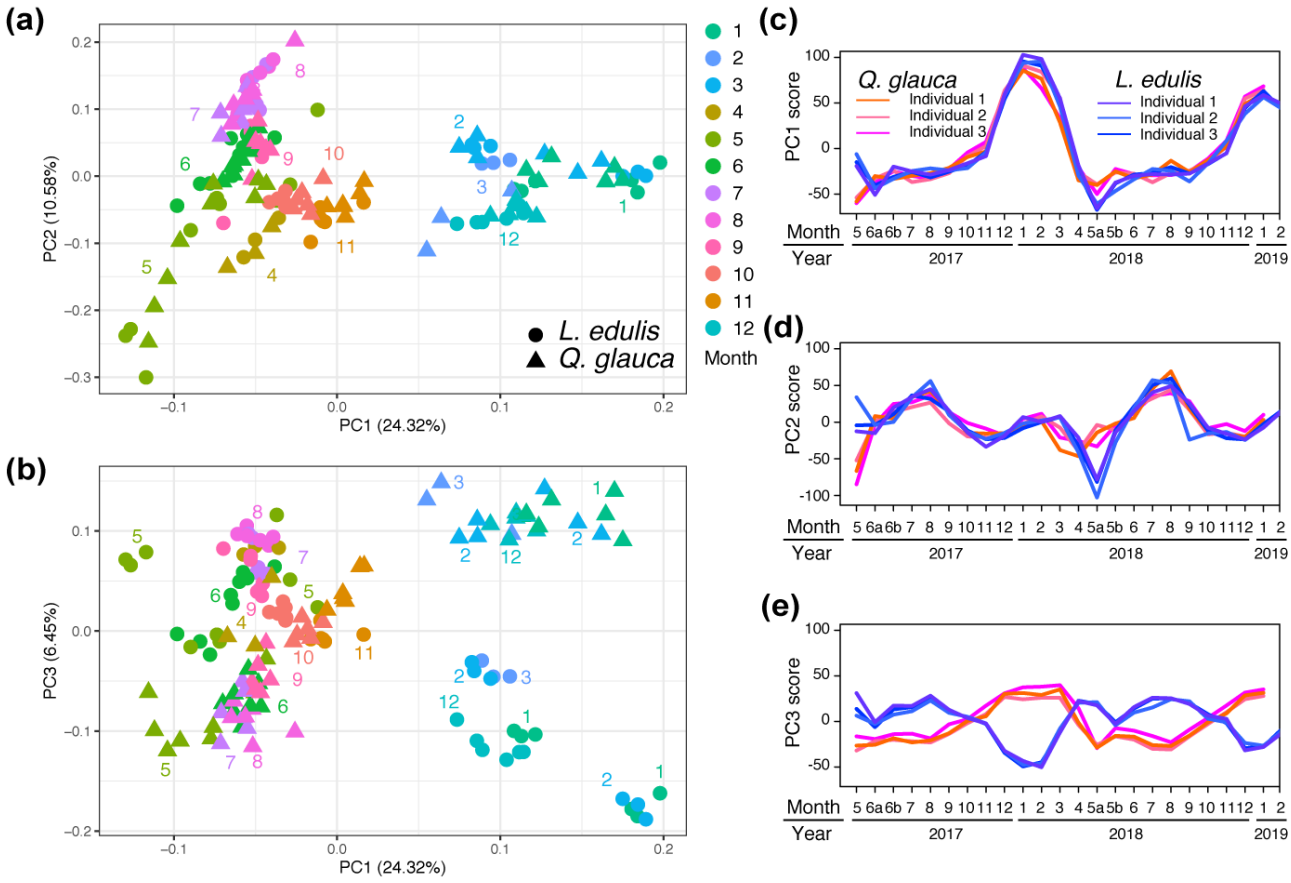

725

726 **FIGURE 4 Major axes of multivariate molecular phenology in *Q. glauca* and *L. edulis*.** Plot of
727 PC2 versus PC1 (**a**) and PC3 versus PC1 (**b**) resulting from the PCA of the 7,707 orthologues for
728 three individuals per species (triangle: *Q. glauca*, circle: *L. edulis*). The numbers indicate the
729 sampling month. The numbers in brackets represent the explained variance. Plot of the PC1 score (**c**),
730 PC2 score (**d**), and PC3 score (**e**) against the month. Expression profiles were monitored in tissues
731 including leaves and buds.

732

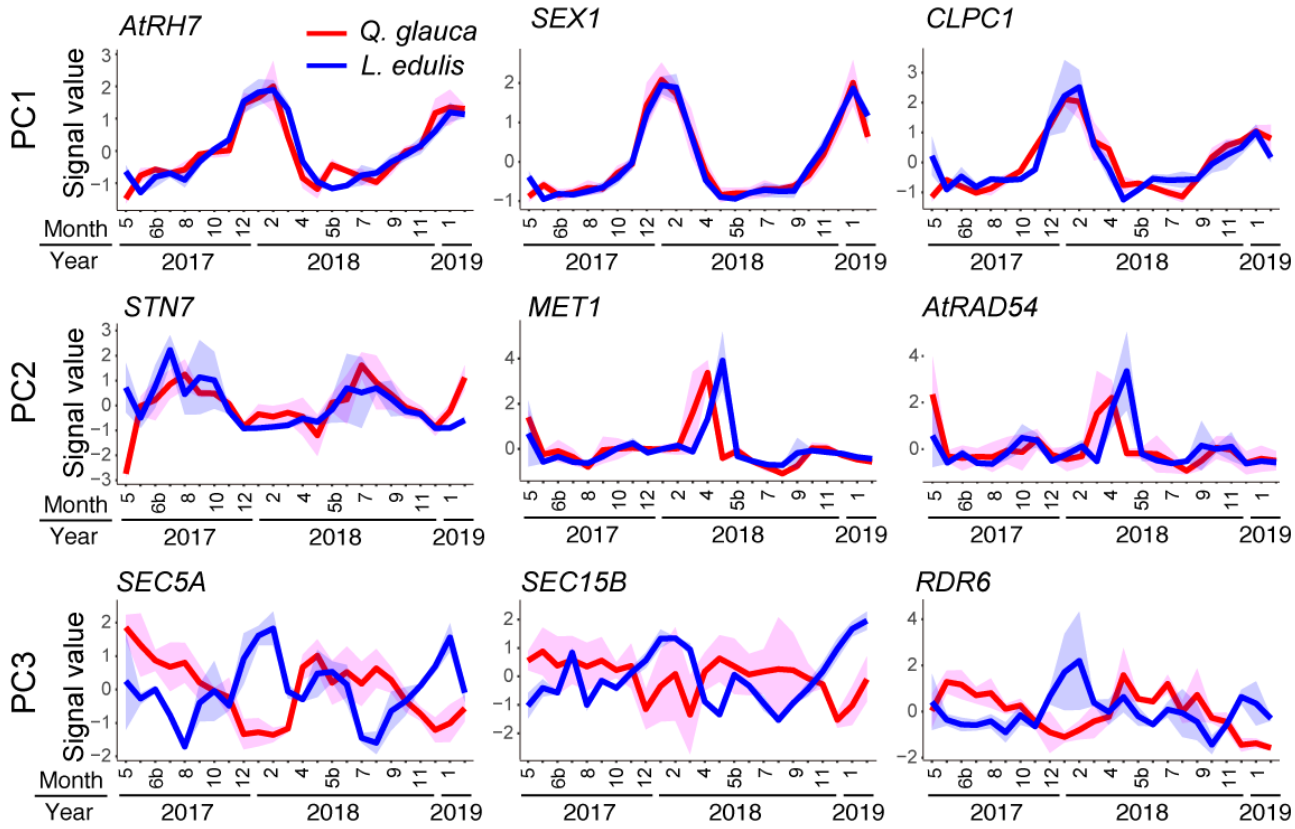

FIGURE 5 Seasonal expression profiles of genes that characterize each of the three axes. Three genes were selected for each of the three axes as examples: PC1 (*AtRH7, SEX1, and CLPC1*), PC2 (*STN7*, *MET1*, and *AtRAD54*), and PC3 (*SEC5A, SEC15B,* and *RDR6*). The two lines indicate signal values for *Q. glauca* (red) and *L. edulis* (blue). The average (line) ± s.d. (envelope) is shown ($n = 3$). Expression profiles were monitored in tissues including leaves and buds.

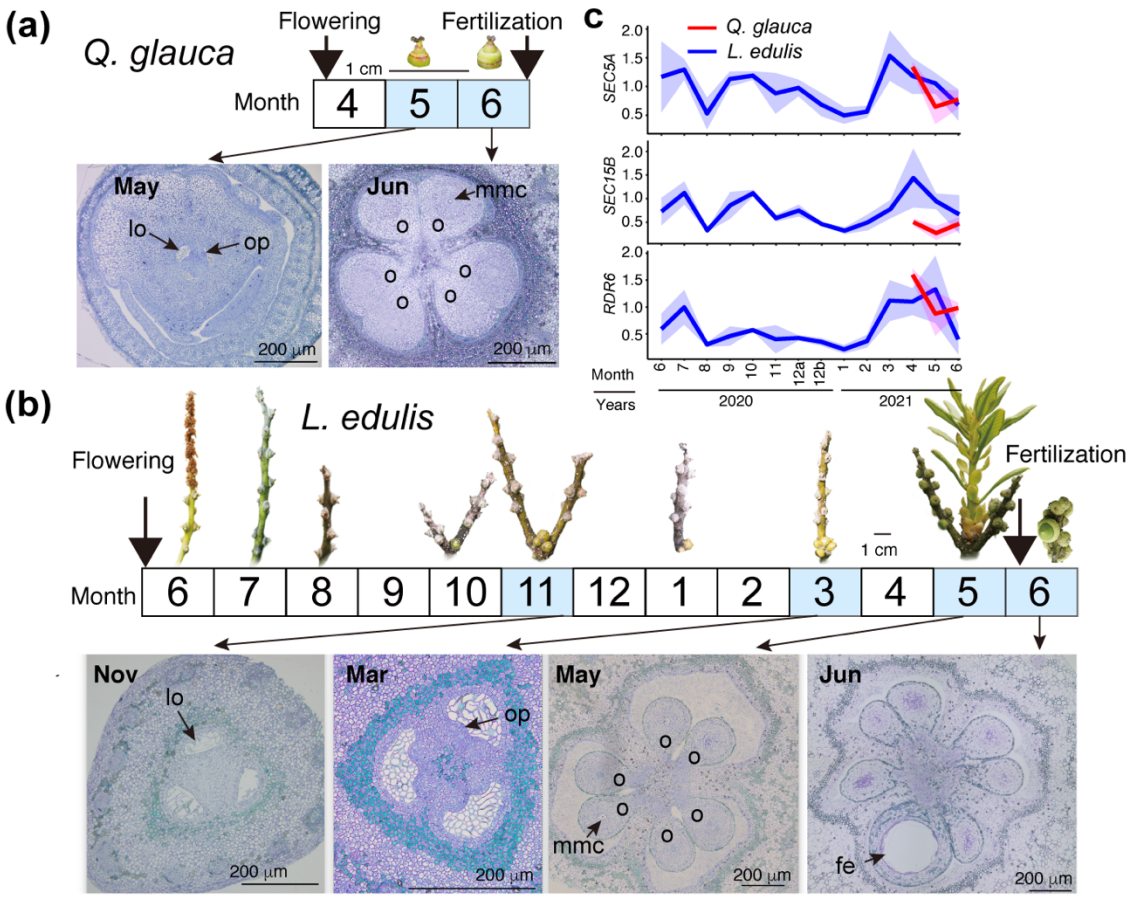

741

742 **FIGURE 6 Ovule development and expression dynamics of candidate genes.** Transverse sections
743 of ovules and image of pistillate flowers of *Q. glauca* (**a**) and *L. edulis* (**b**) collected on November 11
744 in 2018 and March 10, May 23, June 6 in 2019. lo: locule, op: ovule primordia, mms: megaspore
745 mother cell, o: ovule, fe: fertilized egg. **c**, Relative expression levels of *SEC5A, SEC15B,* and *RDR6*
746 (average ± s.d. of three replicates) for *Q. glauca* (red) and *L. edulis* (blue) during 2020–2021 against
747 *UBQ10* as a housekeeping gene.

748